Journal of Physics: Conference Series **363** (2012) 012011 doi:10.1088/1742-6596/363/1/012011

Non-equilibrium "thermal noise" of low loss oscillators

G Karapetyan[1], D Agguiaro[1], M Bonaldi[2,3], L Castellani[1], R Hajj[1], C Lazzaro[1], D Mazzaro[1], M Pegoraro[1], C Poli[1], R Thakur[1], L Conti[1]

[1] INFN, Sezione di Padova, Via Marzolo 8, I-35131 Padova, Italy
[2] Institute of Materials for Electronics and Magnetism, Nanoscience-Trento-FBK Division, I-38123 Povo, Trento, Italy
[3] INFN, Gruppo Collegato di Trento, Sezione di Padova, I-38123 Povo, Trento, Italy

gagik.karapetyan@pd.infn.it

Abstract. The RareNoise project aims at studying how ground-based gravitational wave detector are affected by the thermodynamic non-equilibrium states which are present in their experimental apparatus. We present the RareNoise experimental work which focuses on the study of the 'thermal noise' of low loss oscillators subject to steady-state thermal gradients. We also present the first results of the experimental campaign on steady-state non-equilibrium oscillators around room temperature.

1. Introduction.

Ground-based detectors of gravitational waves (GW) are sophisticated experiments to detect small distortions of the spacetime predicted by general relativity. Ground based ones consist of Michelson laser interferometers with an arm length of up to a few kilometers (VIRGO [1], LIGO and aLIGO [2], GEO600 [3]), or mechanical oscillators with masses of up to several tons [4]. To reach a detection rate of a few events per year, a sensitivity of 10^{-22} in 1*msec* is required [5]. To meet this goal several techniques are proposed and used to lower the contribution of the noise sources; among them thermal noise proves to be difficult to tackle.

Usually GW detectors are considered as equilibrium devices, hence the thermal noise is assumed to have Gaussian distribution. However this picture is not fully justified [6]: in fact non equilibrium states arise for instance in suspended mirrors due to absorbed laser power and thermal compensation technique. In the cryogenic environment planned for LCGT [7, 8] and under consideration for the 3rd generation GW detector [9] these issues are potentially more relevant. However there is not a clear understanding of thermal noise in non equilibrium states.

The RareNoise project aims at studying how the performance of ground-based gravitational wave detectors is affected by the thermodynamic non-equilibrium states which are present in their experimental apparatus [6].

2. Experimental setup.

We have developed an experimental setup to investigate the statistical properties of the thermal noise of mechanical oscillators subject to steady state thermal gradients around room temperature. The setup hosts simultaneously 3 oscillators in vacuum environment (figure 1) with low mechanical noise.

2.1 The oscillators

Each oscillator is machined from a single piece of Al5056, a material with low intrinsic mechanical losses [10]. Basically it consists of a square cross section rod kept in the vertical position, fixed at the top end and loaded by a cuboid mass at the bottom end (Fig. 2). A prototype version of such oscillators is reported in reference [11]. The length of the rod is $0.1m$, cross section is $30.25 \cdot 10^{-6}\ m^2$ and the cuboid mass is about $0.25kg$. These dimensions are chosen after FEM modelling, so that the first longitudinal mode of the part resonates at about $1.4kHz$. In this mode the position of the cuboid mass oscillates along the vertical axis, as the rod elongates and shrinks. The 3 oscillators are identical except for the volume of the cuboid masses: they differ by 5.5% and 11% in volume to separate the resonant frequencies of the longitudinal modes. This is done in order to avoid mechanical couplings of the oscillators. To the same bottom part of the suspension where the oscillators are fixed we also attached piezoelectric actuator to provide for mechanical excitation of the oscillators (see figure 1).

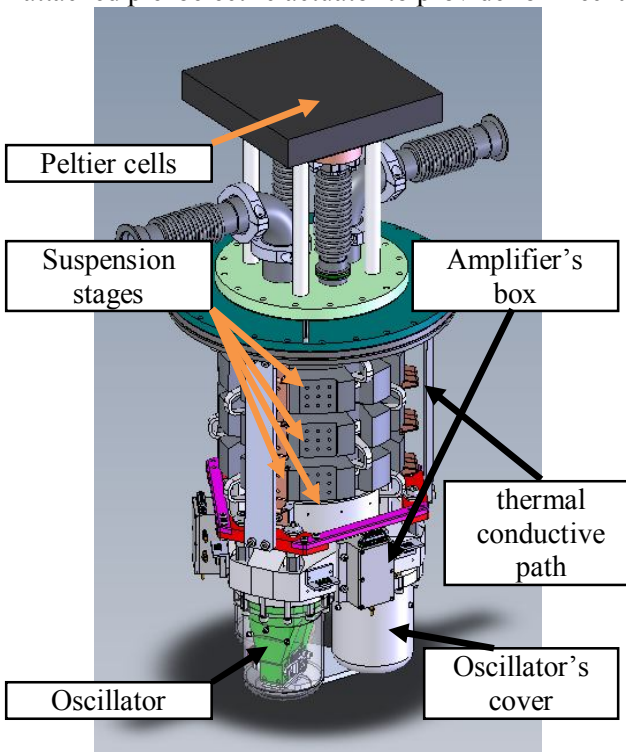

Figure 1. Suspension system with mounted oscillators. Oscillators are inserted into metallic covers for protection while in air.

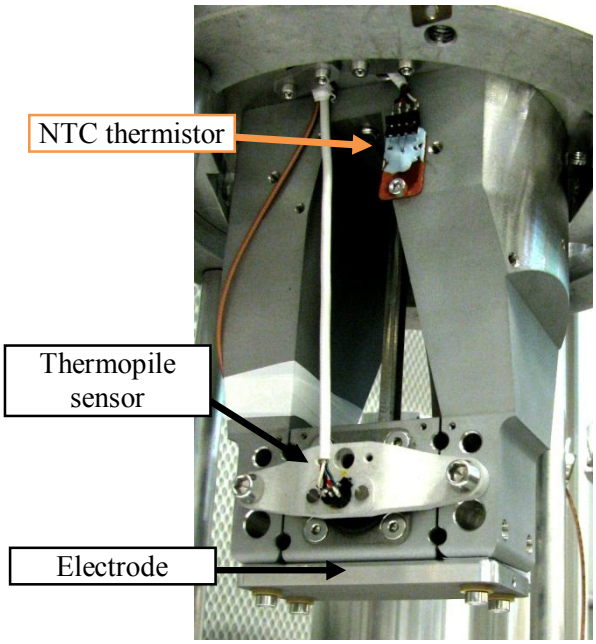

Figure 2. Inside the oscillator's cover.

2.2 The displacement readout.

To measure the oscillations of the cuboid mass each of the 3 oscillators is equipped with capacitive readout. To this end we form a capacitor by facing a Al5056 plate to the bottom surface of the cuboid mass. This plate is supported by two arms parallel to the rod and electrically insulated from them by two Teflon spacers (figure 2). The thicknesses of the spacers range between $100\mu m$ and $300\mu m$. The resulting overall capacitance ranges from $160pF$ to $290pF$. This capacitance is the sum of the capacitance C formed by the plate and the cuboid mass (dielectric medium is the vacuum) and the capacitance C_{teflon} formed by the plate and its support (dielectric medium is Teflon). From the mechanical design we estimate the ratio between these capacitances to be $\frac{C}{C_{teflon}} \approx 3.21$. The facing surfaces of the electrodes and cuboid masses are diamond turned in order to be able to setup electric

fields up to 10^7 *V/m*. In fact working at constant charge the sensitivity of the readout is proportional to the electric field according to the following equation:

$$dV = E_0 \frac{dx}{\left(1 + \frac{C_p}{C}\right)}$$

- where *dx* is the displacement of the cuboid mass, *dV* is the corresponding developed voltage signal and the E_0 is the electric field across the capacitance *C*, and C_p is the sum of C_{teflon} and all parasitic capacitances. In order to reduce the latter we have minimized the length of the wire between the readout and the amplifier by placing it in the vacuum chamber close to the oscillator (see figure 1); we estimate the parasitic capacitances to be about 10*pF*. Each of the 3 amplifiers is custom made and adds a (single sided) noise contribution of about 6 $nV/Hz^{-1/2}$ in the frequency range of interest: from 0.3*kHz* to 2*kHz*. The amplifiers are designed as band pass filters with gain G=100 in the range of interest (see figure 3).

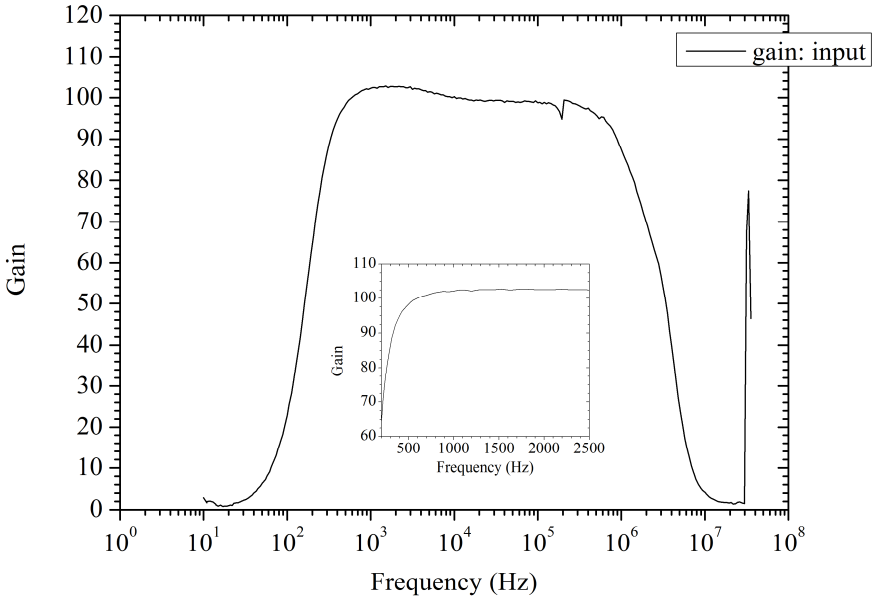

Figure 3. Voltage gain measurement one of the 3 (identical) amplifiers. The inset is a zoom in the range of 200-2500 Hz.

2.3 Mechanical suspension

To reduce mechanical noise in the setup we suspend oscillators and amplifiers by a cascade of active and passive filters; the active filter is provided by an air suspended platform which supports all the experimental apparatus. The passive suspension consists of a cascade of 4 mechanical filters effective in all directions and housed inside the vacuum chamber: a prototype version of the filters is reported in reference [11]. Overall we estimate to achieve vibration isolation of more than 200*dB* at 1.5*kHz* in all spatial directions. To avoid introducing mechanical noise we pump the vacuum chamber by vibration free ion pump. The pressure level in the chamber is below 10^{-5}*mbar*.

2.4 Thermal control

As mentioned our goal is to study the oscillator thermal noise in non equilibrium steady states due to thermal differences. Thus we need to control the temperature T_1 of the top end of the oscillator rods and the temperature T_2 of each cuboid mass. The control of T_1 is achieved by stabilizing the temperature of the aluminium mass at the end of the suspension cascade and where all oscillators are fixed to. This is achieved by feedback loop that controls the current flowing through Peltier cells placed on the top of the vacuum chamber. To reduce the thermal time constant of this loop we provide thermal conductive path in parallel to the mechanical filters. The resulting time constant is about 12 hours. To be able to set thermal differences across the oscillators we heat the cuboid masses radiatively with thermal sources. This way we are able to set thermal differences up to 15*K* by flowing

about $1W$ power. To measure temperatures of the cuboid masses without adding mechanical losses we use thermopiles while for T_1 we use NTC thermistors (see figure 1,2). To improve radiative coupling we attached graphene coated plates to the two opposite faces of the cuboid masses facing respectively the thermal source and the thermopile (see figure 2).

2.5 Data acquisition.

The outputs of the amplifiers are acquired by a system that can sample simultaneously up to 4 channels at high speed and 16 channels at low speed in continuous mode. For the amplifier output we use 24-bit resolution ADC NI PXI-4462 DAQ at $8kSamples/sec$ within $\pm 300mV$ range. All temperature sensors and environmental monitor signals are acquired at $0.1Sample/sec$ by NI 9219 24-bit universal analog inputs. The development platform of the acquisition system was chosen to be NI LabView. During the acquisition it also provides live data view from the oscillators. Data storage is arranged in proprietary binary data format: the header is the 10sec time average of each environmental signal and the body consists of *80000* samples of the amplifier signals. Data analysis is implemented with ROOT libraries [12].

The feedback control program of T_1 interacts with acquisition of the temperature sensors. It reads T1 measurement, computes the correction signal with PID algorithm for a given temperature set point and controls via Ethernet a Sorensen XTR850 DC power supply connected to the Peltier cells. The power supply to the thermal sources of the oscillators and for the thermopiles is provided by NI PXI-4110 dc power supply.

3. Experimental results.

Before starting experimental runs in non equilibrium steady states we perform test runs for diagnostics. Figure 4 is an example of the power spectral density of the amplifier output with $E_0=1.2\cdot 10^7\ V/m$.

Up to $200Hz$ dominant noise source is mechanical noise, also amplified by suspension resonances. Above $200Hz$ the amplifier noise becomes dominant. A few peaks are still present due to mains harmonics. At about $300Hz$ transverse modes of the oscillator are present. The inset shows the zoom around the resonance of the longitudinal mode at $1348Hz$. Red curve is lorentzian fit of the resonance:

$$f(x) = y_0 + A\frac{w}{4(x-x_c)^2 + w^2}$$

where x_c is resonance frequency, w is full width at half maximum and A is the curve area times $2/\pi$. From the fit we infer the oscillator quality factor $Q = \frac{x_c}{w} = 4380$. From the curve area we compute equivalent noise temperature of the oscillator as:

$$T = \frac{(2\pi)^3 A\, m\, x_c^2}{4k_B E_0^2 G^2}\left(1 + \frac{C_p}{C}\right)^2$$

where m is the mass of the longitudinal mode, which we approximate as the cuboid mass $0.25kg$. The resulting noise temperature is $230K$ which is in agreement with the temperature of $288K$ measured by the thermometers within the error bars. These are mainly due to estimation of the electric field and mode mass. This result shows that the oscillator is dominated by thermal noise. Similar results we get with the other oscillators.

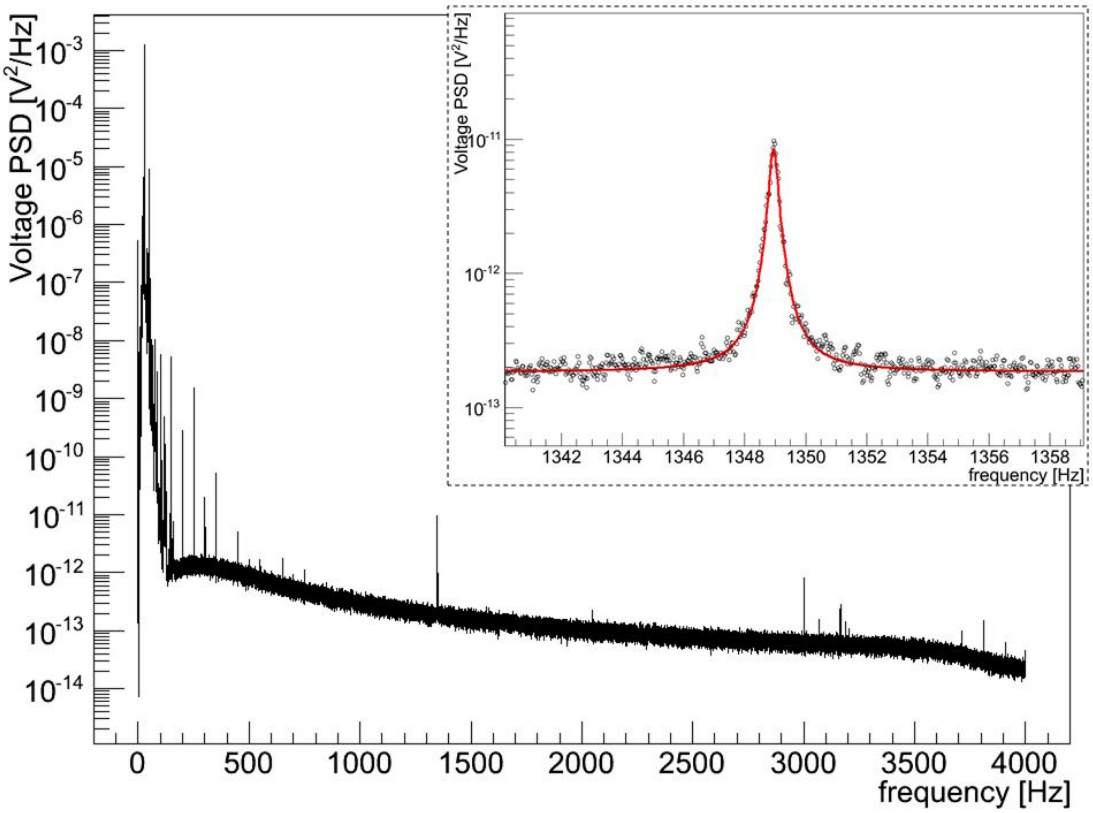

Figure 4. Power spectral density of the amplifier output for one of the oscillators in equilibrium. The inset is the zoom around the resonance of the longitudinal mode of the oscillator. The black points represent experimental data and the red solid line is the lorentzian curve that best fits the data. The decrease of the noise level above 3500*Hz* is due to the anti-alias filter in the acquisition system.

4 . Conclusions.

We have developed a system capable to make thermal noise measurements of the macroscopic mechanical oscillators around 1.4*kHz*. The thermal profiles of the oscillators can be actively controlled: this system is ready to be used for experimental campaign to thermal noise of the oscillators in non-equilibrium steady states.

References

[1] B Caron *et al* - 1997 *Class. Quantum Grav.* **14** 1461 doi:10.1088/0264-9381/14/6/011
[2] https://www.advancedligo.mit.edu/summary.html
[3] B Willke *et al* - 2002 *Class. Quantum Grav.* **19** 1377 doi:10.1088/0264-9381/19/7/321
[4] L Ju *et al* - 2000 *Rep. Prog. Phys.* **63** 1317 doi:10.1088/0034-4885/63/9/201
[5] The gravitational wave international committee roadmap – June 2010, http://gwic.ligo.org/roadmap/
[6] L. Conti *et al.* – 2010 *Class. Quantum Grav.* **27**, 084032
[7] S Miyoki *et al* - 2004 *Class. Quantum Grav.* **21** S1173 doi:10.1088/0264-9381/21/5/116
[8] T Uchiyama *et al* - 2004 *Class. Quantum Grav.* **21** S1161 doi:10.1088/0264-9381/21/5/115
[9] http://www.et-gw.eu/
[10] P. W. Adams *et a*l - 1991 *Rev. Sci. Instrum*. **62**, 2461
[11] Mario Saraceni *et al* - 2010 *Rev. Sci. Instrum.* **81**, 035115
[12] http://root.cern.ch/drupal/